Maghemite nanoparticles bearing di(amidoxime) groups for the extraction of uranium from wastewaters

Cite as: AIP Advances **7**, 056702 (2017); https://doi.org/10.1063/1.4973436
Submitted: 21 September 2016 . Accepted: 10 October 2016 . Published Online: 27 December 2016

Eva Mazarío, Ahmed S. Helal, Jeremy Stemper, Alvaro Mayoral, Philippe Decorse, Alexandre Chevillot-Biraud, Sophie Novak, Christian Perruchot, Claude Lion, Rémi Losno, Thierry Le Gall, Souad Ammar, Jean-Michel El Hage Chahine, and Miryana Hémadi

Maghemite nanoparticles bearing di(amidoxime) groups for the extraction of uranium from wastewaters

Eva Mazarío,[1] Ahmed S. Helal,[1,2] Jeremy Stemper,[3] Alvaro Mayoral,[4] Philippe Decorse,[1] Alexandre Chevillot-Biraud,[1] Sophie Novak,[1] Christian Perruchot,[1] Claude Lion,[1] Rémi Losno,[5] Thierry Le Gall,[3] Souad Ammar,[1] Jean-Michel El Hage Chahine,[1,a] and Miryana Hémadi[1,a]

[1]*ITODYS – Interfaces, Traitements, Organisation et Dynamique des Systèmes, Université Paris Diderot, Sorbonne Paris Cité, CNRS-UMR, 7086, France*
[2]*Nuclear Materials Authority, P.O. Box 540 El Maadi, Cairo, Egypt*
[3]*CEA Saclay, iBiTec-S, Service de Chimie Bioorganique et de Marquage, Bât. 547, F- 91191 Gif-sur-Yvette, France*
[4]*Instituto de Nanociencia de Aragón (INA) - Universidad de Zaragoza, Spain*
[5]*Institut de Physique du Globe de Paris, Sorbonne Paris Cité, UMR 7154, CNRS, F-75005 Paris, France*

(Presented 1 November 2016; received 21 September 2016; accepted 10 October 2016; published online 27 December 2016)

Polyamidoximes (pAMD) are known to have strong affinities for uranyl cations. Grafting pAMD onto the surface of functionalized maghemite nanoparticles (MNP) leads to a nanomaterial with high capacities in the extraction of uranium from wastewaters by magnetic sedimentation. A diamidoxime (dAMD) specifically synthesized for this purpose showed a strong affinity for uranyl: $K_a = 10^5$ M^{-1} as determined by Isothermal Titration Calorimetry (nano-ITC). The dAMD was grafted onto the surface of MNP and the obtained sorbent (MNP-dAMD) was characterized. The nanohybrids were afterward incubated with different concentrations of uranyl and the solid phase recovered by magnetic separation. This latter was characterized by zeta-potential measurements, X-Ray Photoelectron Spectroscopy (XPS) and X-Ray Fluorescence spectroscopy (XRF), whereas the supernatant was analyzed by Inductively Coupled Plasma coupled to Mass Spectrometry (ICP-MS). All the data fitted the models of Langmuir, Freundlich and Temkin isotherms very well. These isotherms allowed us to evaluate the efficiency of the adsorption of uranium by MNP-dAMD. The saturation sorption capacity (q_{max}) was determined. It indicates that MNP-dAMD is able to extract up to 120 mg of uranium per gram of sorbent. Spherical aberration (C_s)-corrected High-Resolution Scanning Transmission Electron Microscopy (HRSTEM) confirmed these results and clearly showed that uranium is confined at the surface of the sorbent. Thus, MNP-dAMD presents a strong potential for the extraction of uranium from wastewaters. [http://dx.doi.org/10.1063/1.4973436]

I. INTRODUCTION

Uranium is one of the most widely used radioactive elements in civilian power plants.[1] Exposure to this metal with other radioactive elements has dramatically increased after the civil nuclear catastrophes in Europe (Chernobyl) and more recently in Japan (Fukushima Daiichi). These led to the release of large quantities of radioisotopes contaminating soil, vegetation and water. This radioactive pollution constitutes a major health problem with a high social and environmental impact. Uranium is

[a]To whom correspondence should be addressed Email: hemadi@univ-paris-diderot.fr or chahine@univ-paris-diderot.fr

highly toxic in all its oxidation states and causes severe damage to bones, skin and kidney.[2] It is neurotoxic, accumulates in the brain and often leads to cancer.[3] In aqueous solution, uranium is present preferentially in the VI valence state as uranyl ion (UO_2^{2+}). According to the World Health Organization, if the quantity of uranium exceeds 15 μgL^{-1} in drinking water, a cancer risk is inevitable.[4] Therefore, safe handling and disposal of nuclear waste is needed to avoid contamination. In the past decades, several methods, such as chemical precipitation,[5] exchange resins,[6] dialysis,[7] have been investigated and used for the extraction and removal of uranium(VI) from soils and aqueous solutions.[8] Nowadays, solid-phase extraction based on magnetic nanoparticles (NP) is attracting a great deal of attention because they have good stability in a wide pH range and a high surface/volume ratio. Iron oxide nanoparticles are the most investigated magnetic materials, as they are easy to synthesize at low cost. Moreover, they can be collected and removed from a complex multiphase system by an external magnetic field.[9] There are different kinds of iron oxide materials with wide domains of application.[10,11] The most studied polymorphic crystallites are magnetite (Fe_3O_4), maghemite (γ-Fe_2O_3) and hematite (α-Fe_2O_3). In this work, a specifically synthesized diamidoxime (dAMD) (data not published) was grafted onto functionalized maghemite nanoparticles (MNP) to give a sorbent, MNP-dAMD. The choice of ligand was dictated by the fact that this dAMD is known to form highly stable complexes with uranyl.[12] The sorbent system was characterized by Thermogravimetric Analysis (TGA), Zeta potential, High-Resolution Scanning Transmission Electron Microscopy (HRSTEM) and X-ray Electron Spectroscopy (XPS). The efficiency of the free dAMD chelator was determined by nano-Isothermal Titration Calorimetry (nano-ITC). The sorption test and the chelation efficiency of the MNP-dAMD nanohybrid were investigated by X-ray Fluorescence spectroscopy (XRF) and Inductively Coupled Plasma with Mass Spectrometry (ICP-MS). It should be emphasized that our main goal here is to elaborate a sorbent based on MNP-dAMD able to reduce, efficiently confine and remove, radioactive waste, more specifically uranyl, from contaminated water.

II. EXPERIMENTAL SECTION

A. Synthesis and functionalization of maghemite nanoparticles

Maghemite nanoparticles (NP), γ-Fe_2O_3, 10 nm in diameter, were synthetized by the polyol method[13] and then functionalized with 3-aminopropyl-triethoxysilane (APTES).[14] Finally, dAMD was grafted onto the MNP by the formation of an amide bond between the amino groups of MNP and the carboxylic acid groups of the dAMD (FIG. 1).

B. Instrumentation

Nano-ITC was carried out at 25 °C in water at pH 5.8 by using a nano-ITC calorimeter (TA Instruments, USA) with an active cell volume of 0.94 mL and a 250 µL syringe. The power curve (heat flow as a function of time) was integrated by means of the NanoAnalyze program to obtain the overall heat produced during the reaction. All solutions were thoroughly degassed by stirring. Titrations were performed by an automated sequence of 50 injections, each of 5 µL of a uranyl solution (0.4 mM), into the sample cell containing the dAMD solution (0.02 mM). Injections were spaced at 300 s intervals to ensure complete equilibration. Three titrations were carried out for each measurement. The reported data are the best-fit values.

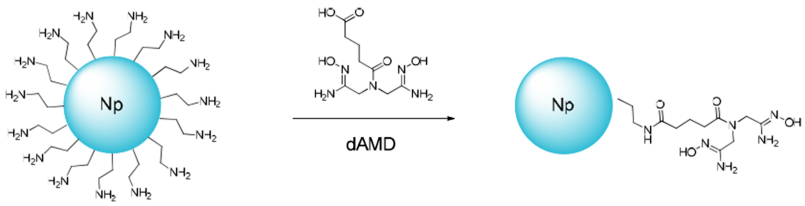

FIG. 1. Scheme of the grafting of dAMD onto MNP.

XPS was performed with an ESCALAB 250, Thermo VG Scientific spectrometer equipped with a monochromatic Al KαX-ray source. The samples were fixed on holders using conducting double-sided adhesive tape and pumped overnight in the fast entry lock prior to transfer to the analysis chamber.

ICP with Mass Spectrometry was performed on an Agilent 7900 Q-ICP-MSICP-MS.

Thermal analyses were performed in a Setaram TGA92 system from room temperature up to 800 °C in air at a heating rate of 20 °C min^{-1}.

Zeta-potentials were measured at pH 5.8, using 10^{-2} M KNO_3 as background electrolyte, on Zetasizer Nano S from Malvern Instruments.

Chemical analysis of Fe and U was performed by XRF using a MINIPAL4 spectrometer equipped with a rhodium X-ray tube operating at 30 kV and 87 μA current emission.

Crystallite size was calculated from the X-ray diffractogram of an as-synthesized sample (XRD, Panalytical x'pert pro) by means of the FullProf suite based on the Rietveld method.

Atomic resolution data coupled with chemical information were recorded in a FEI TITAN probe corrected microscope, which was operated at 300 kV.

C. Sorption and chelation tests

A stock solution of U(VI) (1000 $mg.L^{-1}$) was prepared by dissolving $UO_2(C_2H_3O_2)_2.2H_2O$ in doubly distilled water acidified with nitric acid. Batch experiments were carried out by contact of 5 mg of MNP-dAMD sorbent with 15 mL of uranyl solution at pH 5.8 with uranium concentrations of 0, 20, 40, 60, 80 and 125 $mg.L^{-1}$. The samples were vortexed for 3h at 2000 rpm. Magnetic sedimentation was performed by using a supermagnet (magnetic field of 1.3 T), to separate the supernatant from the solid phase. The solid was dried and analyzed by XRF, XPS and HRTEM. The concentration of uranium remaining in the supernatant was determined by ICP-MS. The equilibrium sorption capacity was determined by equation 1:

$$q_e = \frac{(C_0 - C_e)}{m} xV \tag{1}$$

C_0 ($mg.L^{-1}$), is the initial concentration of uranium; C_e ($mg.L^{-1}$) is the concentration of uranium at the equilibrium after the chelation test; V(L), the volume of the sample and m(g), the mass of the sorbent system. Several isotherm models were used to characterize the sorption mechanism and to determine the saturation chelation capacity (q_{max}).

III. RESULTS AND DISCUSSION

Nano-ITC was used to determine the affinity of dAMD for uranyl cation (since the carboxyl group could take part in complexation, an analogue was actually employed, in which the entire carboxyl group chain was replaced by a benzoyl group). The ITC titration curves of U(VI) binding to (dAMD) are shown in FIG. 2. The heat variation was computed and the values of the thermodynamic parameters were determined [TABLE I; binding enthalpy (ΔH), binding constant (K_a), and stoichiometry (n)]. This heat variation was ascribed to the formation of a complex between U(VI) and dAMD (Eq. 2) with an negative enthalpy (ΔH = -39.9 $kJ.mol^{-1}$) which implies an exothermic process.

$$\text{dAMD} + UO_2^{2+} \rightleftharpoons (\text{dAMD-}UO_2) \tag{2}$$

with

$$K_a = \frac{[(pAMD - UO_2)]}{\left[UO_2^{2+}\right][pAMD]} = 10^5 M^{-1}$$

The affinity constant of dAMD for UO_2^{2+} is comparatively very high.[15] This makes the ligand suitable for grafting onto the surface of MNP for the confinement of U(VI).

NP were synthesized by the polyol method and functionalized by APTES (MNP). The average MNP crystal size was determined by XRD (D_{XRD} = 9.1 ± 0.3 nm, TABLE I). XRD peaks were typical of the spinel structure with no extra phase observed (figure not shown). The size distribution was evaluated and the average MNP size determined by statistical analysis (D_{TEM} = 8.6 ± 1.5 nm, TABLE I).

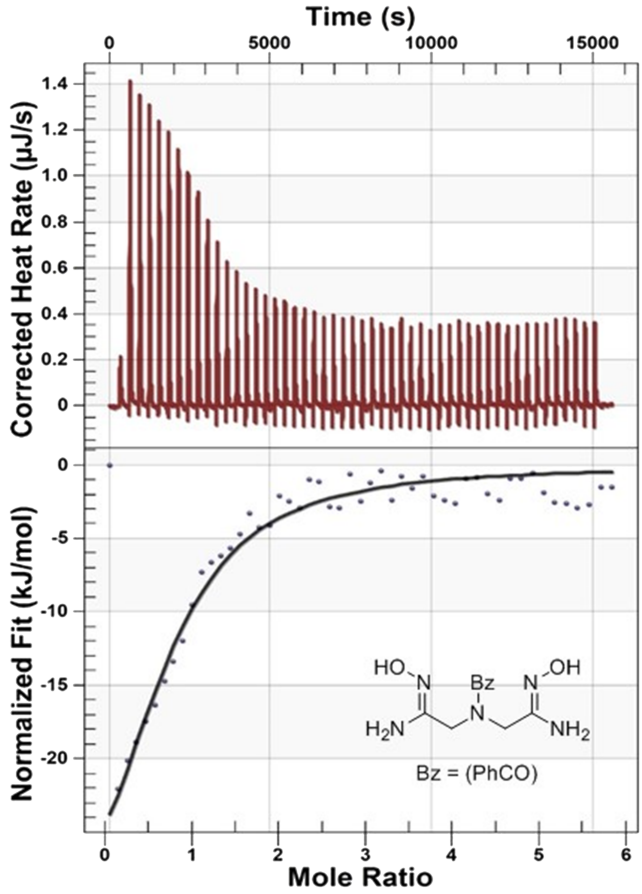

FIG. 2. Nano-ITC) binding curves for complexation of dAMD with U(VI).

The grafting of dAMD onto MNP was characterized by TGA, where a total weight loss of 7.1 % was found (TABLE I). This loss is ascribed to the presence of an organic coating (APTES and dAMD) at the NP surface. By subtraction of the weight loss relative to APTES (5.8 %), the percentage of dAMD at the surface of NP was estimated to be 1.3%. Therefore, taking into account the average diameter of MNP, we estimate that each NP averages 78 molecules of dAMD at its surface, which corresponds to a surface concentration of 0.25 molecules/nm^2. This was confirmed by the zeta-potential with $\zeta = (2.0 \pm 0.7)$ mV at pH 5.8. Indeed, at pH 5.8, ζ varies from +22 mV for MNP to +2.0 mV for MNP-dAMD. This underlines the effectiveness of the grafting.

The concentration of uranium, remaining in the supernatant of the contaminated solution, after MNP-dAMD magnetic recovery, was determined by ICP-MS, and q_e was calculated from equation 1.

The data were correctly fitted by three different models:

1. The Langmuir isotherm describes the adsorption of a monolayer of uranium onto a surface bearing a finite number of identical sites.

$$\frac{C_e}{q_e} = \frac{1}{K_L q_{max}} + \frac{1}{q_{max}} \times C_e \tag{3}$$

From the plot of C_e/q_e against C_e (eq. 3, FIG. 3a), the saturation sorption capacity (q_{max}) is determined and indicates that at pH 5.8, MNP-dAMD extracts up to 120 mg of uranium per gram (TABLE I). This value is higher than that obtained with magnetite nanoparticles either raw[16] or functionalized with quercetin.[17] The value of the Langmuir constant (K_L) is indicative of the good adsorption capacity.[18]

TABLE I. Characterization parameters of MNP-dAMD before and after the chelation tests.

D_{TEM} (nm)		At. % (XPS)		At. % (XRF)	
8.6 ± 1.5	Element	MNP-dAMD	MNP-dAMD (Chelation Test)	Fe	U
D_{XRD} (nm)	C	49.33	44.99	96.95	3.05
9.1± 0.3	Fe	5.12	6.25	ζ-potential (mV) pH 5.8	
Weight Loss (%) (MNP-dAMD)	N	1.65	1.9	MNP MNP-dAMD ITC parameters	22.0±0.4 2.0 ± 0.7
7.1	O	37.35	41.05	log K_a (M^{-1})	5
Molecular Weight dAMD ($gmol^{-1}$)	Si	5.91	4.17	n ΔH ($kJmol^{-1}$)	0.75 -39.9
280	U	-	1.65	ΔG ($kJmol^{-1}$)	-28.6

Isotherm parameters

Langmuir			Freundlich			Temkin	
Q_{max}	K_L	r	n	K_F	r	B_T	r
120 mg /g	0.12	0.99	3.44	3.24 10^1	0.935	21	0.97

2. The Freundlich isotherm (eq. 4, FIG. 3b) describes reversible adsorption and is not restricted to the formation of a monolayer. It is also used to understand the extent and degree of favorability of the adsorption process.

$$\log q_e = \log K_F + \frac{1}{n_F} \log C_e \tag{4}$$

K_F is roughly an indicator of the adsorption capacity mg/g, when $1 < n_F < 10$. In this case, the level of adsorption becomes high.[19] The values of Freundlich isotherm (TABLE I) indicate a strong interaction between the sorbent and the metal.[20] This is probably the result of the highly stable (chemisorption) that occurs between uranyl and dAMD, as shown by nano-ITC.

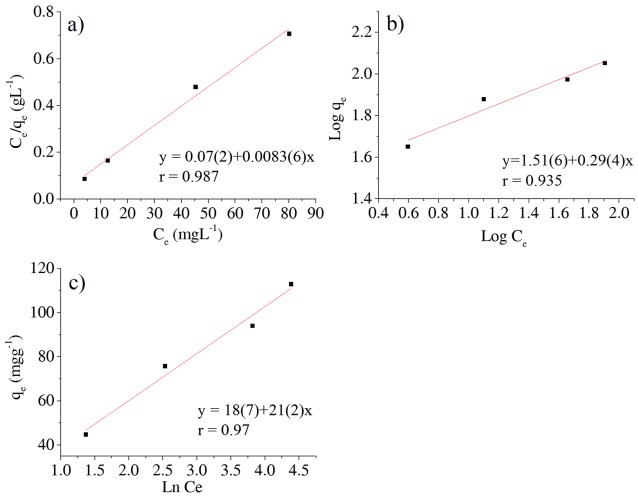

FIG. 3. Plot of: a) Langmuir, b) Freundlich and c) Temkin isotherms for the adsorption of U(VI) onto MNP-dAMD.

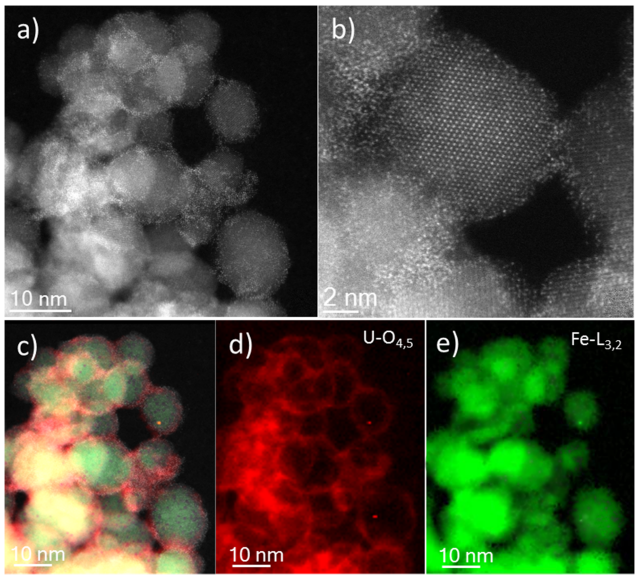

FIG. 4. C_s-corrected STEM-HAADF analysis. a) and b) corresponds to the high-resolution images. c) STEM image with the superimposed U and O signals. d) U-$O_{4,5}$ map and e) Fe-$L_{3,2}$ extracted map.

3. The Temkin isotherm (eq. 5, FIG. 3c) assumes that the free energy of adsorption is a function of the surface coverage.[21]

$$q_e = B_T ln K_T + B_T ln C_e \tag{5}$$

where K_T (L.mg^{-1}) is the equilibrium binding constant and B_T is a constant related to the surface heterogeneity of the MNP-dAMD. This isotherm describes the interaction between sorbent (MNP-dAMD) and adsorbate (UO_2^{2+}). The higher K_T, the higher the heat of adsorption (TABLE 1). This reflects the high affinity of the sorbent for uranyl which again confirms the thermodynamic data obtained by nano-ITC.

Furthermore, XPS analyses were performed on MNP-dAMD before and after incubation with uranyl. TABLE I clearly shows the presence of U with an atomic percentage of 1.65 %. However, the depth of XPS analysis does not exceed 10 nm. Therefore, in order to examine the volume of the particles completely, XRF measurements were performed. They showed that the overall masses of Fe and U are 167.8 and 22.5 µg, respectively. This gives an atomic percentage of about 3.0% for uranium which leads to approximately 650 uranium atoms per NP.

Finally, the C_s-corrected STEM-HAADF (high angle annular dark field), confirmed our results by showing that uranium is confined at the surface of MNP-dAMD (FIG. 4). Under our operation mode, heavy elements appear brighter and the spots on the surface are those of U atoms (FIG. 4a). The good crystallinity of the NPs was corroborated at higher magnification (FIG. 4b), where a 9 nm NP can be observed along the [111] zone axis of the spinel structure. Elements were extracted by Electron Energy Loss Spectroscopy (EELS) analysis. In FIG. 4c, we show the high-resolution STEM image with the U-$O_{4,5}$ (d-red) and Fe-$L_{3,2}$ (e-green) maps superimposed.

IV. CONCLUSION

MNP-dAMD is a good and efficient sorbent for the chelation and confinement of uranium. It very efficiently removes uranium from aqueous solutions, and the contaminated nanoparticles are easily recovered by a simple magnet. Therefore, MNP-dAMD presents a very promising potential for uranium decontamination from wastewaters. A desorption test was performed by incubating MNP-dAMD-Uranyl in an acid solution (HNO_3, 0.1 M) in order to evaluate its capacity for reuse. Preliminary results show that MNP-dAMD is perfectly reusable (at least 10 times) and retains its

magnetic and chelation properties. Further investigations are still required to achieve a full estimate of the system selectivity for uranyl cations.

ACKNOWLEDGMENTS

This work was supported by the National Research Agency program "DECRET" (ANR ANR-13-SECU-0001). The authors are grateful to Dr J. S. Lomas for constructive discussions.

[1] S. S. Wise, W. D. Thompson, A. M. Aboueissa, M. D. Mason, and J. P. Wise, Sr., Chem. Res. Toxicol. **20**(5), 815–820 (2007).
[2] *The health effects of depleted uranium munitions* (Royal Society, document 6/02, 2002).
[3] P. Lestaevel, P. Houpert, C. Bussy, B. Dhieux, P. Gourmelon, and F. Paquet, Toxicology **212**(2-3), 219–226 (2005).
[4] *Guidelines for Drinking Water Quality*, 2nd ed. (WHO, 1998).
[5] I. Doroshenko, J. Zurkova, Z. Moravec, P. Bezdicka, and J. Pinkas, Ultrason. Sonochem. **26**, 157–162 (2015).
[6] C. Gunathilake, J. Górka, S. Dai, and M. Jaroniec, J. Mater. Chem. A **3**, 11650–11659 (2015).
[7] A. J. Semiao, H. Rossiter, and A. I. Schafer, Journal of Membrane Science **348**, 174–180 (2010).
[8] A. Künküla and T. Abbasovb, Powder Technology **149**(1), 23–28 (2004).
[9] D. Feng, C. Aldrich, and H. Tan, Hydrometallurgy **56**(3), 359–368 (2000).
[10] H. Piraux, J. Hai, P. Verbeke, N. Serradji, S. Ammar, R. Losno, N. T. Ha-Duong, M. Hémadi, and J. M. El Hage Chahine, Biochim. Biophys. Acta. **1830**, 4254–4264 (2013).
[11] J. Xie, J. Huang, X. Li, S. Sun, and X. Chen, Curr. Med. Chem. **16**(10), 1278–1294 (2009).
[12] K. Singh, C. Shah, C. Dwivedi, M. Kumar, and P. N. Bajaj, Appl. Polym. Sci. **127**, 410–419 (2012).
[13] H. Basti, L. Ben Tahar, L. S. Smiri, F. Herbst, M. J. Vaulay, F. Chau, S. Ammar, and S. Benderbous, J. Colloid Interface Sci. **341**(2), 248–254 (2010).
[14] H. Piraux, J. Hai, T. Gaudisson, S. Ammar, F. Gazeau, J. El Hage Chahine, and M. Hémadi, J. Appl. Phys. **17**, 17A336 (2015).
[15] X. Sun, G. Tian, C. Xu, L. Rao, S. Vukovic, S. O. Kangd, and B. P. Hayd, Dalton Transactions **43**(2), 551–557 (2014).
[16] D. Das, M. K. Sureshkumar, S. Koley, N. Mithal, and C. G. S. Pillai, J. Radioanal. Nucl. Chem. **285**, 447–454 (2010).
[17] S. Sadeghia, H. Azhdaria, H. Arabib, and A. Z. Moghaddama, J. Hazard. Mater. **215-216**, 208–216 (2012).
[18] T. W. Webber and R. K. Chakkravorti, AIChE Journal **20**(2), 228–238 (1974).
[19] M. G. Mahfouz, A. A. Galhoum, N. A. Gomaa, S. S. Abdel-Rehem, A. A. Atia, T. Vincent, and E. Guibal, Chem. Eng. J. **262**, 198–209 (2015).
[20] A. D. Site, J. Phys. Chem. Ref. Data **30**, 187 (2001).
[21] H. K. Boparai, M. Joseph, and D. M. O'Carroll, J. Hazard. Mater. **186**, 458–465 (2011).